ADVANCED MATERIALS

Supporting Information

for *Adv. Mater.*, DOI: 10.1002/adma.201203051

A New Class of Room-Temperature Multiferroic Thin Films with Bismuth-Based Supercell Structure

*Aiping Chen, Honghui Zhou, Zhenxing Bi, Yuanyuan Zhu, Zhiping Luo, Adrian Bayraktaroglu, Jamie Phillips, Eun-Mi Choi, Judith L. MacManus-Driscoll, Stephen J. Pennycook, Jagdish Narayan, Quanxi Jia, Xinghang Zhang, and Haiyan Wang**

ADVANCED MATERIALS

Supporting Information

for Adv. Mater., DOI: 10.1002/adma.201203051

A New Class of Room Temperature Multiferroic Thin Films with Bismuth Supercell-based Structure

*Aiping Chen, Honghui Zhou, Zhenxing Bi, Yuanyuan Zhu, Zhiping Luo, Adrian Bayraktaroglu, Jamie Phillips, Eun-Mi Choi, Judith L. MacManus-Driscoll, Stephen J. Pennycook, Jagdish Narayan, Quanxi Jia, Xinghang Zhang, and Haiyan Wang**

Submitted to ADVANCED MATERIALS

Supporting Information for

A New Class of Room Temperature Multiferroic Thin Films with Bismuth Supercell-based Structure

By *Aiping Chen, Honghui Zhou, Zhenxing Bi, Yuanyuan Zhu, Zhiping Luo, Adrian Bayraktaroglu, Jamie Phillips, Eun-Mi Choi, Judith L. MacManus-Driscoll, Stephen J. Pennycook, Jagdish Narayan, Quanxi Jia, Xinghang Zhang,* and *Haiyan Wang**
* Email: wangh@ece.tamu.edu

I. Experimental Section

Thin Film Growth. Pulsed laser deposition (PLD) was employed to grow epitaxial BFMO nanocomposite films on LAO (001) and STO (001) substrates. The composite target, with a 1:1 molar ratio of $Bi_{1.05}FeO_3$ and $Bi_{1.05}MnO_3$, was obtained by conventional ceramic sintering process. The substrate temperature ranged from 600~750 °C and oxygen pressure of 100~200 mTorr were maintained for the depositions. After deposition, the films were in-situ annealed for 1 hour at 400 °C in an oxygen pressure of 300 Torr before cooling down to room temperature at a cooling rate of 5 °C/min. The films with thickness from 10 nm to 300 nm were deposited. A number of films were made by varying the deposition temperature, laser repetition frequency, deposition duration and different buffer layers and substrates. The optimum growth conditions for high purity layered BFMO phase were at a growth temperature of 700 °C and a laser pulse rate of 2 Hz. CeO_2 buffer layer was deposited at 700°C with a thickness of 10~20 nm between the BFMO films and substrates. XRD results show BFMO thin films directly deposited on STO substrates are pseudo-perovskite structure and the ones directly on LAO are the new Super-Cell (SC) structure with a thin self-assembled interlayer. BFMO films present the bismuth SC structure on both LAO and STO if a thin epitaxial CeO_2 buffer layer was inserted between the film and substrate, as shown in Figure S1 (a) and (b), respectively.

Microstructural Characterization. The microstructures of the films were examined by X-ray diffraction (XRD) (BRUKER D8 powder X-ray diffractometer, and Panalytical MRD PRO x-ray diffractometer) and transmission electron microscopy (TEM) (JEOL JEM-2010 and FEI Tecnai G2 F20). The scanning transmission electron microscopy (STEM) images were taken by using a VG HB603U STEM equipped with Nion aberration corrector operating at 300 kV.

Magnetic Measurements. The magnetic properties of the films were systematically investigated by the vibrating sample magnetometer (VSM) mode on a commercial Physical Properties Measurement System (PPMS 6000, Quantum Design). During the magnetic measurements, the out-of-plane magnetizations were measured by applying a magnetic field perpendicular to the film plane the in-plane magnetizations were recorded by applying a magnetic field parallel to the film plane. In the FC measurements, the samples were put in a field followed by cooled down to 10 K and then increased to 350 K, and the magnetizations were measured during the heating cycle. Substrate contribution has been removed from the results.

Electrical Measurements. The piezoelectric properties were measured at ambient conditions with a conductive Pt-Ir coated Si tip (Model: SCM-PIT) in the Veeco Dimension NanoMan atomic force microscope (AFM). Piezoelectric hysteresis loop were performed in piezoresponse mode at 17 kHz, which is far below the resonance frequency of the cantilever (60±10 kHz), with ac voltage amplitude of 5~10 V, and a deflection setpoint of 0.6 V. The spring constant K (1.75±0.02 N/m) and deflection sensitivity (65±5 nm/V) was calibrated in the contact mode with the tip on a silicon wafer. In order to characterize the ferroelectric properties of BFMO with double bismuth SC structure, a thin CeO_2/ $SrRuO_3$ (SRO) buffer layer was deposited between BFMO and STO and tested to be a successful bottom electrode.

Thus, capacitors with Pt (200 nm)/BFMO (130 nm)/CeO_2 (15 nm)/SRO (15 nm)/STO (001) and Pt (200 nm)/BFMO (130 nm)/CeO_2 (15 nm)/Nb:STO (001) configurations were used for the piezoelectric properties and *P-E* hysteresis loop measurements. Top electrodes with 350 μm×350 μm size were deposited by magnetron sputtering through a shadow mask. The ferroelectric hysteresis loop was conducted by a commercial TF Analyzer 1000 from aixACCT.

II. Microstructure of BFMO SC gorwn on CeO_2 buffered substrates

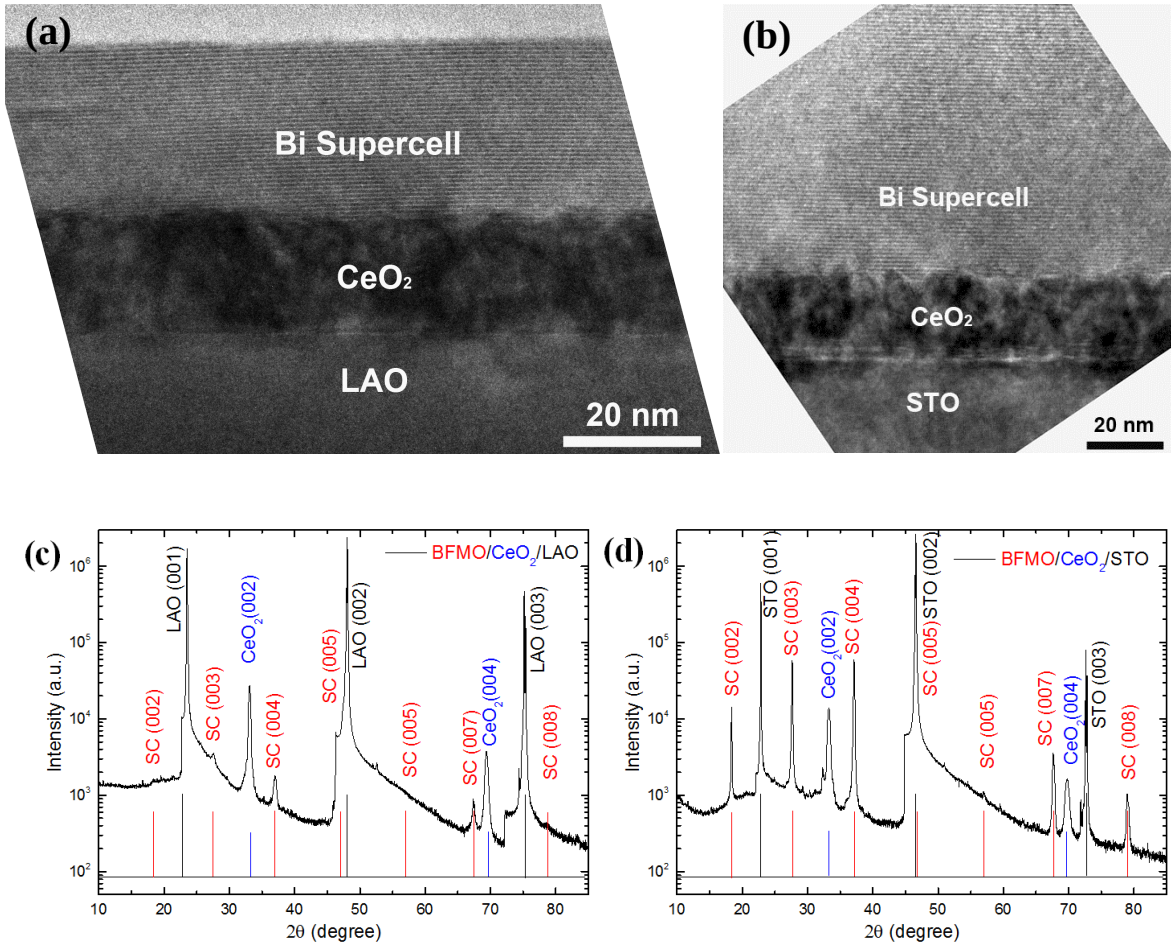

Figure S1.TEM of BFMO SC grown on CeO_2 buffered (a) LAO and (b) STO substrates. XRD patterns of BFMO SC on CeO_2 buffered (c) LAO and (d) STO substrates.

III. Cation ratio of the BFMO SC structure

Cation ratio of the BFMO films with double bismuth SC structure has been studied by TEM-EDX (Oxford Instruments ATW type EDS detector with INCA Energy TEM platform for chemical analysis of element with Z >= 5). STO substrate has been selected as the reference for the EDX analysis and the Sr/Ti ratio is close to 1 (Table 1). The BFMO deposited on the STO substrate is a conventional double perovskite phase Bi_2FeMnO_6 with slightly bismuth deficiency (about 9 % estimated from the EDS analysis above). However, the BFMO film grown on the LAO yields a cation ratio of Bi : Fe : Mn = 3 : 2 : 2, suggesting a further loss of bismuth compared to the conventional phase (Table 3). It has to point out that there are usually 4 % ~ 7 % unidentified phases exist in the BFMO322 SC phase from the XRD results. Also the cation ration of the SC is evaluated based on the atomic model build from the STEM images (Figure S2). Considering one unit cell, there are eight bismuth atoms on the conner (shared by other eight neighboring unit cells; so 1/8 belongs to this unit cell), twelve on the edge, fourteen on the face and thirteen within the unit cell, resulting in a total of 24 bismuth atoms for one unit cell. Similarly, there are in total 34 transitional metal (Fe or Mn) atoms in one unit cell. Since the distribution of Fe an Mn is complete random confirmed by the SAED study, the ratio among Bi:Fe:Mn in one unit cell is 24 : 16 : 18 (or 24:18 :16, depends on where one starts to count), approximated to 3 : 2 : 2, consist with the EDS analysis on the BFMO film grown on the LAO.

Table 1. Cation ratio in $SrTiO_3$. (All results in atomic %)

Spectrum	O	Ti	Sr
Spectrum1	49.61	25.69	24.70
Spectrum2	57.87	21.64	20.49
Mean	**53.74**	**23.66**	**22.60**
Std. deviation	5.84	2.86	2.98
Max	57.87	25.69	24.70
Min	49.61	21.64	20.49

Table 2. Cation ratio in regular BFMO on STO substrates with perovskite structure. (All results in atomic %)

Spectrum	O	Mn	Fe	Bi
Spectrum 1	58.66	10.29	11.30	19.75
Spectrum 2	63.55	9.26	9.73	17.47
Spectrum 3	58.94	10.50	11.15	19.41
Mean	**60.38**	**10.01**	**10.73**	**18.88**
Std. deviation	2.74	0.66	0.87	1.23
Max.	63.55	10.50	11.30	19.75
Min.	58.66	9.26	9.73	17.47

Table 3. Cation ratio in BFMO322 with SC structure. (All results in atomic %)

Spectrum	O	Mn	Fe	Bi
Spectrum 1	63.16	11.11	8.62	17.11
Spectrum 2	67.23	9.00	9.08	14.69
Spectrum 3	65.11	9.76	8.85	16.27
Spectrum 4	62.17	11.12	10.72	15.99
Spectrum 5	62.85	10.42	9.09	17.64
Spectrum 6	64.68	10.80	12.26	12.25
Spectrum 7	65.23	10.58	11.78	12.41
Spectrum 8	61.96	11.58	12.47	13.99
Mean	**64.05**	**10.55**	**10.36**	**15.04**
Std. deviation	1.82	0.83	1.64	2.05
Max	67.23	11.58	12.47	17.64
Min	61.96	9.00	8.62	12.25

IV. Possible structural origin of the BFMO SC structure

The BFMO SC structure is possibly derived from Aurivillius phase, for the sharing similarities in the Bi_2O_3 planes. Taking one of the simplest Aurivillius phase, Bi_2WO_6,[1] for example, as illustrated in Figure S2(a), the Bi_2WO_6 structure presents typical alternative stacking of the $(Bi_2O_2)^{2+}$ slabs and the $(A_{m-1}B_mO_{3m+1})^{2-}$ perovskite-like layer (here m = 1, B is occupied by W^{6+}). In Figure S2(b), the new BFMO SC under [100] zone axis could be

considered as a layered structure with a systematic stacking fault of missing every other Bi_2O_2 planes of the Bi_2WO_6 lattice. Admittedly, this way of out-of-plane defective stacking might has high energy and not stable; as demonstrated in the article, further structural modulations (Figure 3 in the manuscript) were observed in the SC and may attribute to stabilize the new phase.

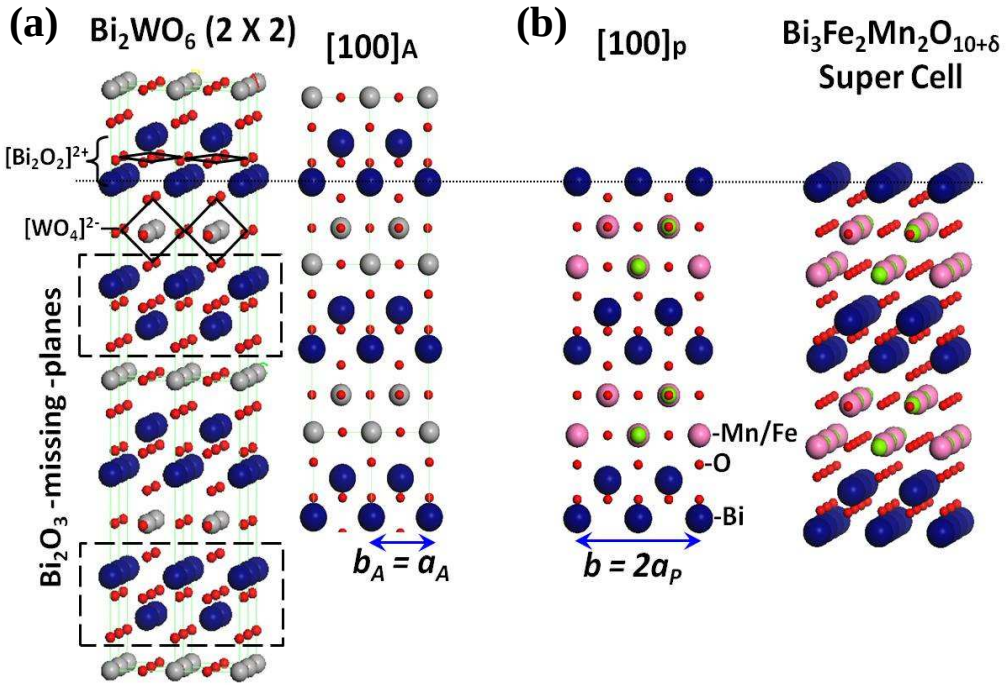

Figure S2. (a), The 2×2 Bi_2WO_6 atomic structure and the layered structure with the stacking fault of missing every other Bi_2O_2 planes are projected along $[100]_A$. (b), The atomic structure of $Bi_3Fe_2Mn_2O_{10+\delta}$ SC along the $[100]_P$ zone axis.

References

[S1] R. W. Wolfe, R. E. Newnahm, *Solid State Commun* **1969**, *7*, 1797.